Deformation mechanisms in TiN/(Ti,Al)N multilayers under depth-sensing indentation

Carvalho, NJM; De Hosson, JTM

Published in:
Acta Materialia

DOI:
10.1016/j.actamat.2005.12.010

Publication date:
2006

Available online at www.sciencedirect.com
SCIENCE DIRECT
Acta Materialia 54 (2006) 1857–1862
Acta MATERIALIA
www.actamat-journals.com

Deformation mechanisms in TiN/(Ti,Al)N multilayers under depth-sensing indentation

N.J.M. Carvalho, J.Th.M. De Hosson *

Department of Applied Physics, Materials Science Center and Netherlands Institute for Metals Research, University of Groningen, Nijenborgh 4, 9747 AG Groningen, The Netherlands

Received 28 April 2005; accepted 8 December 2005
Available online 10 February 2006

Abstract

TiN/(Ti,Al)N multilayer coatings prepared by physical vapour deposition onto steel substrates were subjected to depth-sensing indentation testing. The investigation was aimed at predicting their performance by identifying the contact-induced fracture mechanisms. Analysis of the load–displacement curves showed their efficiency in identifying the occurrence of cracking, the mechanisms of which were explored using new techniques based on focused ion beam cross-sectional transmission electron microscopy of the indents. The fracture modes were observed to take place along the columnar boundaries and in the layers parallel to the interfaces. Furthermore, the load capacity and the transitions between the different deformation regimes were controlled by a combination of the properties of the coating material itself, the substrate upon which the coating was deposited, and the interface(s) that bonded the system together. Nanoindentation testing with a continuous stiffness module and a high-load cell was also used to study the variation of hardness and effective modulus between the multilayer system and a monolithic TiN reference coating.

Keywords: Nanoindentation; Transmission electron microscopy; Scanning electron microscopy; Multilayers; Hardness

1. Introduction

Multilayers with layer dimensions on the nanometre scale can be precisely engineered; these multilayers have new structural features and improved mechanical properties to respond to specific service requirements. A strong impetus has been given to the investigation of TiN/(Ti,Al)N multilayers in relation to the more traditional monolithic TiN films due to their improved wear resistance, hardness, and higher oxidation resistance at elevated temperatures.

Despite much research on the development of multilayer coatings with superior mechanical and tribological properties, questions still remain about the mechanisms, operating at the smallest length scales, underlying the mechanical response. The wear resistance is often attributed to the high hardness as well as to good chemical stability. The achievement of high hardness and high toughness ought to be linked to the large number of internal interfaces, which act as sites of energy dissipation and crack deflection. It is suggested by several authors [1,2] that blunting of crack tips can be controlled by a combination of plastic deformation with strong interfaces and crack deflection occurring due to the elastic mismatch between the layers and differences in their morphology.

However, limited data have been published in order to justify the mechanisms of enhancing the properties of multilayer coatings taking into consideration their microstructural features. This paper describes the results of an investigation to determine the relationship between microstructure, deformation mechanisms, and mechanical properties of multilayers subjected to nanoindentation. To this end, commercially available TiN/(Ti,Al)N multilayer coatings were chosen. Detailed investigations on the residual stress state and microstructure of such coatings have been

* Corresponding author.
E-mail address: j.t.m.de.hosson@rug.nl (J.Th.M. De Hosson).

1359-6454/$30.00
doi:10.1016/j.actamat.2005.12.010

presented previously [3]. In the present work, nanoindentation experiments have been utilized to obtain mechanical property data and an insight into the fracture phenomena of the coating/substrate systems. By combining load–displacement data with observation of indentations in cross-section, using scanning electron microscopy (SEM) and transmission electron microscopy (TEM), important aspects of the contact-induced fracture mechanisms of the coated systems have been revealed.

2. Experimental

The coatings examined in this paper were deposited onto stainless steel (AISI 304) and cold work tool steel (AISI D2) substrates, which were polished to mirror finish surfaces with an average roughness, R_a, value of ≈50 nm. They were provided, and are commercialized, by Balzers AG, Liechtenstein. The deposition parameters were close to, or identical with, those used for production. The deposition process took place in a BAI 830 PM coating unit utilizing a hybrid process described in detail elsewhere [4]. In essence, it combines reactive ion plating deposition of TiN by high current density plasma beam evaporation and reactive magnetron sputtering for the deposition of (Ti,Al)N from a titanium–aluminium alloy target. The deposition process consisted of evacuating the vacuum chamber to a pressure less than 5×10^{-4} Pa, then heating the substrates to a temperature of ≈450 °C to outgas the surfaces. The substrates were then sputter etched (Ar^+) with a negative substrate bias of 1000 V. The coating deposition occurred at 450 °C with a constant partial pressure of N_2. A total thickness of 3.0 μm was aimed at for the coatings. It should be pointed out at the outset that the aim of this paper is to provide a better understanding of the intrinsic relationship between the microstructure and the deformation mechanisms of multilayers grown by commercially available processes. Therefore, questions concerning detailed deposition parameters and reproducibility should be addressed to the manufacturer.

Depth-sensing indentation was used as the principal mechanical testing technique, using a sharp Berkovich tip. The experiments were conducted using an MTS Nano indenter® XP. This instrument has additional functionalities that allow high load measurements, up to 10 N, and a continuous stiffness measurement (CSM) where the contact stiffness is measured continuously as a function of displacement along with the load. With the CSM method stiffness data were collected and subsequently used in calculations of the hardness and modulus. A standard approach – load–unload cycle was used, where the load was held constant at peak load, to allow for compensation of creep, and at 70% of maximum load on unloading for the calculation of any thermal drift effects. The measurements were repeated at least 20 times and were all loaded using a constant strain rate, $\dot{P}/P$, of 0.05 s^{-1}. This procedure permits large numbers of data points to be accumulated in the low-load segment, particularly useful when undertaking experiments on coated systems. The Oliver and Pharr [5] method was used to analyze the experimental data.

SEM and TEM were used to study the microstructure of the as-deposited coatings and the deformed regions around the indents. The analyses were performed using a Philips-XL30(s)-FEG SEM instrument and JEOL 4000 EX/II (operating at 400 kV) and JEOL 2010 FEG (operating at 200 kV) TEM instruments. Cross-sections of the indents for SEM and TEM characterization were prepared using either the method described in detail elsewhere [6] or a focused ion beam (FIB) FEI Strata 235 DB dual-beam workstation. The technique for specimen preparation using the FIB consisted of first milling two crosses alongside the indented area, acting as markers, and then depositing a 1 μm thick layer of platinum to protect the area of interest from Ga^+ ion beam damage and implantation. Material was removed from both sides of the selected area using an ion current of 5 nA, followed by successive thinning steps using decreasing currents from 3 nA to 300 pA until the foil was about 1 μm thick. Subsequently, the bottom and one side of the foil were cut free while tilting the sample at an angle of 45° to the ion beam. A central area containing the indentation apex of a few micrometres in length was then chosen and thinned further to a thickness of 300 nm, leaving at the sides thicker areas that prevented the foil from collapsing. Finally a small area of interest was selected and thinned until electron transparency was achieved. The transfer of the specimen from the sample holder to the TEM grid with a carbon membrane was made ex situ using the electrostatic force of a glass needle. The novelty of this method compared to the more conventional ones frequently reported in the literature [7,8] is that it allows the preparation of cross-sectional TEM specimens from thin films, highly deformed and in a high compressive residual stress state, without their breaking up due to stress relaxation during the final thinning process [9].

3. Results and discussion

3.1. Microstructure and deformation mechanisms under indentation

Detailed studies of the microstructure and deformation mechanisms of physical vapour deposition coatings by cross-sectional observations are still very rare owing to the relatively limited access to transmission electron microscopes and the complexity of the necessary cross-sectional specimen preparation. Since most coatings are heterogeneous materials and deposited on a different substrate material, the differential thinning that occurs on either side of the interfaces might lead to misleading interpretation of the observations. However, the information obtained from cross-sections allows the characterization of coating–substrate interfaces and the microstructural evolution throughout the coating thickness. Further, cross-sections of nanoindentations allow the assessment, on a nanometre

scale, of the contact-induced deformation mechanisms of coated systems. Previously, a technique was developed to cross-section indents for observation using either SEM or TEM [10]. This allows the simultaneously preparation of several indents with different loads and the resulting TEM specimens have a large electron transparency area of uniform thickness. A drawback of such a technique is that the preparation is very time consuming. In recent years, FIB workstations have been used for the preparation of cross-sectional TEM specimens. The advantage of using this technique for cutting through nanoindentations is the efficiency in localizing the specific site and the short preparation time (~2–3 h). For large indents and highly stressed materials this technique is not very suitable, since often the specimens are not evenly thin and the stress relaxation leads to undesirable cracking, masking the deformation mechanisms due to nanoindentations.

In the present study, cross-sections of indents were obtained using both techniques, the former being used for larger indents (higher loads) and the latter for reduced indentation loads. The multilayers exhibited a columnar microstructure that was not disrupted by the multilayer interfaces. The average column diameter increased with film thickness from ~80 nm at the coating–substrate interface up to ~150 nm at the top of the film. From selected area electron diffraction analysis it could be concluded that the columnar grain boundaries were of high angle, since the patterns obtained from adjacent columns showed no clear crystallographic relationship. The interface between the interlayer and the substrate showed an abrupt transition, and at the substrate side dark contrast areas were observed due to strain fields. These were associated with defects within the matrix of the substrate grains induced by residual radiation damage as a result of intense ion irradiation during ion etching.

The deformation mechanisms occurring in TiN single crystals have been studied in the past either by TEM or by calculating the crystallographic anisotropy using Schmid's law [11,12]. The primary slip system for dislocation glide in TiN crystals, which are typically ionic, has been characterized by plastic deformation on {1 1 0} planes with slip occurring along the ⟨1 1 0⟩ directions. (Ti,Al)N has the same *B*1 NaCl crystal structure as TiN. However, the slightly higher hardness of (Ti,Al)N (see below) suggests a more pronounced covalent bonding character, and consequently it should deform under compression along the {1 1 1} planes. The Burgers vector of the dislocations in both materials should be in the ⟨1 1 0⟩ directions, since it corresponds to the shortest distance between either two anions or cations. Given the reactive sputtering deposition nature of the films investigated here, their growth-generated dislocation density overshadowed the dislocation lines in the strain fields formed under the indent. Further, the imaging of the dislocations was beset with difficulties due to the preferential nucleation on inhomogeneities in the film beneath the surface where the shear stress had a maximum value.

The fracture mechanism of the polycrystalline multilayer was considered by cross-sectioning the indents with different peak loads and by observing in detail the deformed regions under the indents using SEM and TEM. Fig. 1 shows cross-sectional SEM images of the multilayer deposited on tool steel and stainless steel substrates and indented by a Berkovich tip with a 500 mN peak load.

A comparison of the film thickness at the indentation apex, where the compressive stress and plastic deformation are expected to be highest, with that far way indicates a direct proportionality of the compressive strain of the multilayers with the indentation depth. The values ranged from ~5% at an indentation depth of 15% of the total coating thickness to ~11.5% at an indentation depth of 67% thickness. In the case of coatings deposited on tool steel substrates (see Fig. 1(a)), a value of about 7% was found. Whenever deposited on stainless steel substrates, the multilayers exhibited a constant compressive strain of ~5% irrespective of the indentation depth, as shown in Fig. 1(b). These results indicate that the relative hardness values of the multilayer and substrates play an important role in the definition of the microstructural responses. Substrates with a higher yield stress will delay plastic deformation, and as a result the multilayer accumulates elastic strain energy leading to an increase of elastic strain energy density. Hence, an increase of compressive strain with

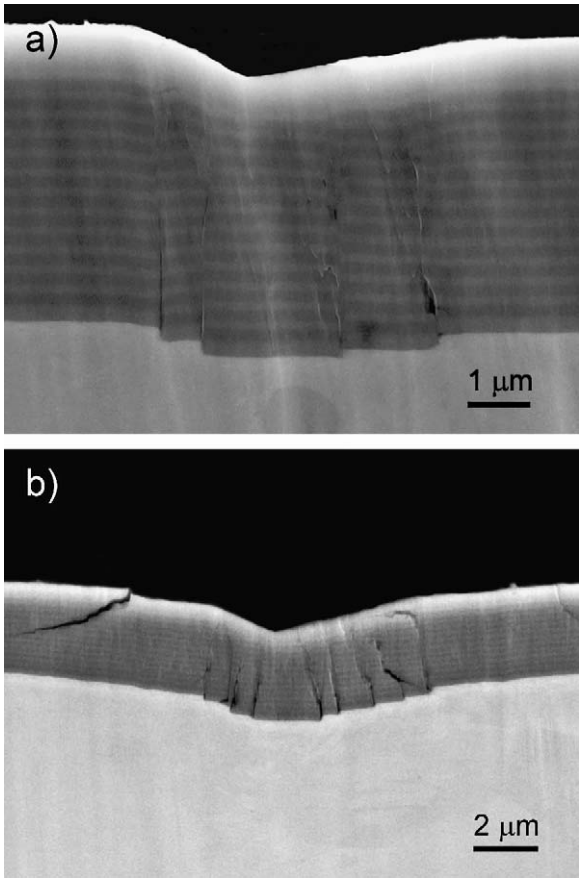

Fig. 1. Cross-sectional SEM images of a 500 mN indent. Coating deposited (a) on tool steel substrate and (b) on stainless steel substrate.

indentation load occurs. For stainless steel, the multilayer is initially compressed in the normal direction but as soon as the indentation contact pressure reaches the low yield stress on the substrate it behaves like a perfectly elastic medium, transferring the indentation load directly to the substrate, which in turn deforms plastically.

The extensive plastic deformation of the substrates and the inability of the coatings to accommodate such deformation during loading lead to a concentration of tensile radial stresses at the coating–substrate interface. There release occurs by brittle crack propagation towards the surface at the columnar grain boundaries due to the shear sliding of adjacent columns under the indentation edges. This process also minimizes the shear loading. The crack tips close as the propagation approaches the zone of compression near the top surface of the impression. This process might be particularly effective for strain energy dissipation, hence avoiding premature failure by delamination of the coating along the interface with the substrate, which is an important mode of failure in tribological applications. The regular displacement was found to be associated with steps (pop-in) observed in the load–displacement curves. Thus it can be argued that the appearance of the first pop-in event is related to the onset of plastic flow in the steel substrate. This reasoning is in line with the commonly used rule of thumb, where the properties of the 'film only' are measured for indentation depths less than 10% of the film thickness, since the first pop-in event is observed to take place at higher penetration depths, where the substrate plays a considerable role in the system deformation behaviour. Fig. 2(a) shows also the presence of lateral cracks located below the indentation impression. They are thought to originate on unloading of the indentation cycle, and tend to propagate approximately parallel to the layers releasing the elastic strain energy stored during bending. The inefficiency of the interfaces of the multilayer in obstructing or deflecting the cracking during unload of the indenter is suggested to be related to the reduced lattice mismatch between the layers and the small variation of the chemical composition across the interface. Thus, it is not surprising to observe transgranular cracking across several columnar grains, being deflected only when intersecting an existing columnar shear crack. The deleterious effect of droplets whenever incorporated in the multilayer can be observed when they are present underneath an indentation impression. The weak columnar boundaries of the macroparticle and the voided region beneath the droplet act as preferential sites for crack nucleation and propagation during the unloading of the indent.

A different cracking mode was observed at the surface layer within the periphery of the indentation impression. In this region the stress distribution is expected to be compressive, in contrast to the interface with the substrate where a tensile state prevails [13]. As can be seen in Fig. 2(b), the centre of the impression is characterized by shallow cracks that run along the columnar grain boundaries. The tangential traction that occurs during loading

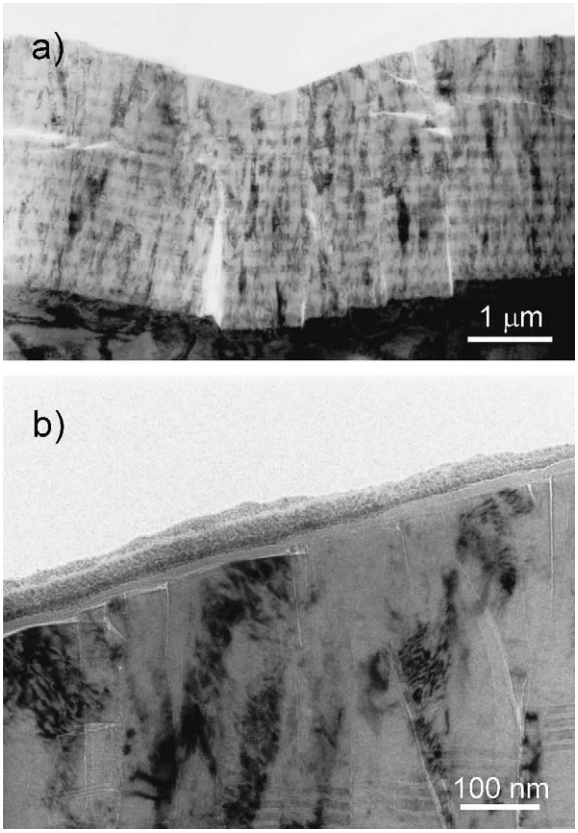

Fig. 2. Cross-sectional TEM bright-field images displaying the crack paths in a coating deposited on stainless steel. (a) Overview showing lateral cracking originating from unloading of the indentation cycle; (b) cracking along the columnar grain boundary located at the surface layer within the indentation impression.

at the surface of adjacent columns leads to their relatively vertical displacement and the generation of shear steps. In contrast to the other failure modes, the shear steps are in a region of high hydrostatic compression and thus are considered to be of mode II (sliding) corresponding to longitudinal shearing of the columnar boundaries in a direction normal to the crack front [14]. The scale of damage induced by the frictional traction is correlated with the columnar diameter.

Cross-sectioning of low peak load indents was intended to characterize the deformation mechanisms within the columnar grains. Fig. 3 displays TEM bright-field images and diffraction patterns of 50 mN indents on multilayers grown on tool steel substrates. In Fig. 3(a), it can be seen that the columnar grains are bent at the edges of the indent and cracking at their boundaries has occurred. Nevertheless, the multilayer stacking has not been disrupted, as happens for higher loads, indicating that most of the plastic deformation is accommodated by the (Ti,Al)N top layer in the region immediately under the indent. The macroscopic deformation of the layer is reflected in the crystal rotation on the microscopic scale. Fig. 3(b) shows two grains with strong diffraction contrast within a column situated under the indenter tip. Observation of the columnar

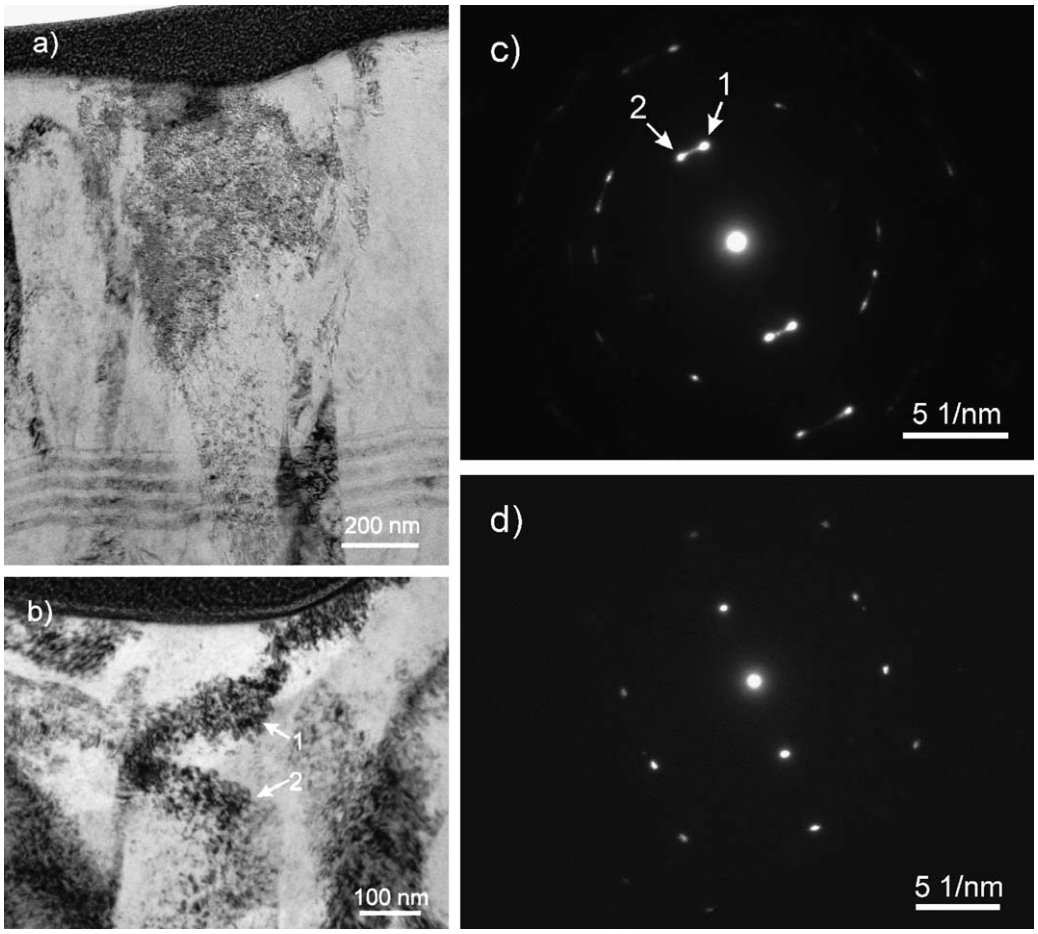

Fig. 3. (a) Overview TEM bright-field image of a cross-section of a 50 mN indent on TiN/(Ti,Al)N deposited on tool steel. (b) Deformation within a column beneath the indentation apex. (c) Selected-area diffraction pattern showing the tilt of crystallographic planes under the indenter tip. (d) Selected-area diffraction pattern away from the indenter for comparison with (c).

structure outside the indented area shows that grains within a column have the same orientation throughout its thickness. However, in this case the diffraction pattern taken with an aperture of similar diameter to the column shows the streaking of the diffraction spots corresponding to rotation of the crystallographic planes, as seen in Fig. 3(c). The diffraction pattern obtained under the same conditions outside of the indented area clearly shows no deformation of the top layer (see Fig. 3(d)). Dark-field imaging has confirmed that each side of the streaked spot corresponds to the tilted upper and lower grains (labels 1 and 2 in Figs. 3(b) and (c), respectively). This phenomenon of rotation of the crystallographic planes has been reported previously by Molina-Aldareguia et al. [15], and can be interpreted as a mean of plastic yield of the (Ti,Al)N layer. Therefore, it follows from the above discussion that no cleavage fracture occurred in these coatings and the deformation mechanism was intergranular fracture.

3.2. Mechanical properties

In Fig. 4(a), hardness values as a function of the displacement normalized to the coating thickness, calculated by depth-sensing indentation, are shown for TiN/(Ti,Al)N and TiN. The increase in hardness observed for shallow displacements is thought to result from uncertainties in the tip end-shape calibration whereas the larger scatter is primarily due to the surface roughness of the as-deposited coatings. For penetration depths of the order of a few hundred nanometres the influence of the substrate on the composite hardness values is much reduced. The hardness of the multilayers at low displacements is slightly higher than that of the monolithic layer. This effect might be related to the higher covalence of the bonds in the (Ti,Al)N layer or to a hardening effect caused by the large number of interfaces parallel to the substrate surface. By assuming that at an indenter penetration of 200 nm the influence of both tip-shape irregularities (the tip radius is 40–50 nm) and substrate (penetration depth less than one-tenth of coating thickness) are negligible, it is possible to estimate the coating hardness for TiN and TiN/(Ti,Al)N to be of the order of 31 and 34 GPa, respectively. The mean effective Young's modulus for TiN and TiN/(Ti,Al)N coated systems as a function of the displacement normalized to the coating thickness is shown in Fig. 4(b). The values were also derived from the continuous stiffness measurements. The

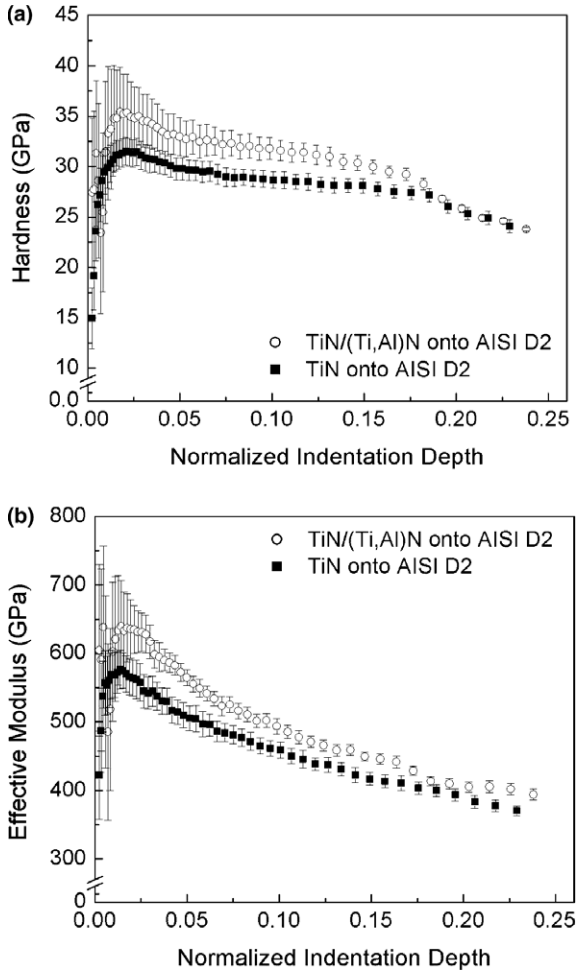

Fig. 4. Hardness and effective Young's modulus values as a function of the displacement normalized to the coating thickness for TiN/(Ti,Al)N and TiN deposited on tool steel substrates.

effective modulus values decrease markedly with increasing displacement into the coated system. The substrate influence is observed at smaller penetration depths, because the long-range component of the elastic field starts extending rather earlier into the more compliant substrate.

4. Conclusions

Multilayer TiN/(Ti,Al)N coatings deposited onto steel substrates by physical vapour deposition were evaluated using depth-sensing indentation in terms of the relationship between microstructure, deformation mechanism, and mechanical properties. The use of load–displacement data and specific procedures for the preparation of cross-sections of nanoindentations with different peak loads have been shown to be valuable for the assessment of the contact-induced deformation mechanisms of coated systems. The effect of the substrate compliance on the fracture of the coatings was investigated using cold work tool steel and stainless steel substrates. The former, stiffer than the latter, induced an increased elastic strain energy density in the multilayers, and hence a higher compressive strain. Different deformation mechanisms were observed to take place depending on the indentation contact pressure. For the highest contact load studied, 500 mN, the main fracture mechanism consisted of brittle crack propagation from the coating–substrate interface towards the surface, along the columnar grain boundaries due to the shear sliding of adjacent columns. It is interesting that this mechanism prevented delamination of the coating along the interface with the substrate. In contrast, when the multilayer was indented at low peak loads, 50 mN, the deformation mechanism was characterized by plastic yielding of the top layer, revealed through rotation of the crystallographic planes within the grains of the columnar structure.

The hardness and effective Young's modulus of the multilayer and monolithic TiN were estimated using the continuous stiffness option provided with the nanoindenter. The results showed that the multilayer exhibits slightly higher values, which is thought to be due to either the higher covalence of the bonds in the (Ti,Al)N layer or to a hardening effect related to the large number of interfaces present in the coating.

Acknowledgements

The work described in this paper was funded by the Netherlands Institute for Metals Research. The authors are grateful to V.G.M. Sivel of the Netherlands Institute for Metals Research for the FIB preparation. The deposition of the coatings on steel substrates by the Balzers Group is acknowledged.

References

[1] Chan KS, He MY, Hutchinsson JW. J Mater Sci Eng 1993;167:57.
[2] Evens MY. Int J Solids Struct 1994;31:3443.
[3] Carvalho NJM, Zoestbergen E, Kooi BJ, De Hosson JThM. Thin Solid Films 2003;429:179.
[4] Bergmann E. US Patent 4877505; 1989.
[5] Oliver WC, Pharr GM. J Mater Res 1992;7:1564.
[6] Carvalho NJM, De Hosson JThM. J Mater Res 2001;16:2213.
[7] Overwijk MHF, Van den Heuvel FC, Bulle-Lieuwma CWT. J Vac Sci Technol B 1993;11:2021.
[8] Dai JY, Tee SF, Tay CL, Song ZG, Ansari S, Er E, et al. Microelectron J 2001;32:221.
[9] Sivel VGM, Alkemade PFA, Carvalho NJM, De Hosson JThM, Zandbergen HW [submitted].
[10] Carvalho NJM, De Hosson JThM. Mater Res Soc Symp Proc 2002;697:P1.5.
[11] Odén M, Ljungcrantz H, Hultman L. J Mater Res 1997;12:2134.
[12] Hayashi T, Matsumuro A, Watanabe T, Mori T, Takahashi Y, Yamuguchi K. JSME Int J A 2001;44:94.
[13] Johnson KL. Contact mechanics. Cambridge: Cambridge University Press; 1985.
[14] Bhowmick S, Kale AN, Jayaram V, Biswas SK. Thin Solid Films 2003;436:250.
[15] Molina-Aldareguia JM, Lloyd SJ, Oden M, Joelsson T, Hultman L, Clegg WJ. Philos Mag A 2002;82:1983.